D4

RECIPROCATING MAGNETIC REFRIGERATOR

Dean L. Johnson

Jet Propulsion Laboratory,
California Institute of Technology,
Pasadena, CA, USA

The Jet Propulsion Laboratory is developing a 4-15 K magnetic refrigerator to test as an alternative to the Joule-Thomson circuit as the low temperature stage of a 4-300 K closed-cycle refrigerator. The reciprocating magnetic refrigerator consists of two matrices of gadolinium gallium garnet spheres located in tandem on a single piston which alternately moves each matrix into a 7 tesla magnetic field. A separate helium gas circuit is used as the heat exchange mechanism for the low and the high temperature extremes of the magnetic refrigerator. Details of the design and results of the initial refrigerator component tests are presented.

Key words: Closed cycle refrigerators; expansion engine; gadolinium gallium garnet; gas pumps; magnetic refrigeration.

1. Introduction

In the past few years a lot of interest has been generated towards designing and developing a continuously operating 4 K magnetic refrigeration stage for a closed cycle refrigerator (CCR) [1-4]. Its potential for high efficiency performance makes magnetic refrigeration a likely alternative to the passively operating, but highly inefficient Joule-Thomson circuit. The success of the magnetic refrigerator for this temperature range will depend on the development of suitable design approaches to answer questions of heat transfer effectiveness, helium gas movement, wear rates of materials and expected life cycles of the refrigerator components.

The Jet Propulsion Laboratory (JPL) has initiated the development of a 4-15 K magnetic refrigerator to assess its potential as a replacement to the Joule-Thomson circuit of a closed cycle refrigerator [5]. JPL has been using 1 Watt at 4.5 K closed cycle refrigerators since 1965 for cooling the low-noise maser amplifiers required to receive very weak signals from spacecraft in deep space. Up to 30 CCRs are in near continuous operation in the Deep Space Communications Network that JPL operates for the National Aeronautics and Space Administration. These CCRs log approximately one quarter of a million hours annually. The successful development of a magnetic refrigerator would reduce the overall life-cycle costs of the CCR by reducing the electrical power consumption of the CCR and by insuring a longer MTBF for the operating refrigerator.

The design of the engineering model 4-15 K magnetic refrigerator under development at JPL addresses the basic requirements of refrigeration power, DC field stability, reliability and efficiency. It is the objective of this paper to describe the design of the magnetic refrigerator, discuss the component test results, and provide a status of the development effort.

2. Experimental design

Choice of the magnetic refrigerator design must depend ultimately on the device it is to cool, in this case the maser, an ultrasensitive microwave signal amplifier whose performance depends critically on a stable DC magnetic field, and on a low operating temperature having milliKelvin stability. The refrigerator package for the maser must be orientation independent since it is located in the feedcone of a large tracking antenna which points anywhere from horizon to zenith. The design requirements for the magnetic refrigeration system is therefore quite stringent. The design of the engineering model presently under development addresses only the basic requirements of refrigeration capacity, DC field stability, reliability and efficiency. The reciprocating design has been selected for its relative' simpler fabrication requirements and the greater ease with which the experimental results could be verified theoretically.

The schematic of the magnetic refrigerator design is shown in figure 1. All components have been fabricated at JPL. The major components are shown in figure 2. The CTI Model 1020 expansion engine provides the high temperature heat sink for the magnetic refrigerator and is capable of producing better than 9 W of refrigeration at 15 K. This refrigeration capacity is a major determining factor in the final 4 K cooling power of the magnetic refrigerator. The hydrogen heat switch is used during initial cooldowns to precool the helium dewar and magnet assembly to 20 K before liquid helium is transferred into the dewar. This experimental design presently calls for the external transfer of liquid helium to cool the magnet; future designs will require the magnetic refrigerator stage to provide the parasitic refrigeration requirements of the magnet.

The 7 T magnetic field is supplied by a 10.2 cm NbTi solenoid having a 6.3 cm bore. The magnet is operated in persistent mode. When the magnet is fully charged, the current leads will be detached at the magnet to minimize heat leak into the liquid helium bath. Quench protection of the magnet is provided by a short length of stainless tubing attached across the magnet leads and immersed in the liquid helium bath. The magnet is encased with a magnetically soft material, Hiperco (Carpenter Technology Corp., Reading, PA), having a saturation induction of 2.4 T. The Hiperco is used to entrap much of the magnetic flux exiting from the bore of the magnet.

The piston is driven with a 185 W (1/4 H-P) speed-controllable gearmotor. This rotational motion is converted to reciprocating motion by means of a "ball reverser" (Norco, Inc., Georgetown, CT), a nut with ball bearings that run in a cross-hatched track cut into the drive shaft. The track has a set stroke length of 9.2 cm and provides a displacement of 3.175 cm/2π rad. A 10 rad/s rotation rate for the gearmotor translates to a 5.1 cm/s linear speed for the GGG piston and to a cycle frequency of 0.28 Hz. A turn-around in the ends of the track automatically reverse the direction of travel of the nut to provide smooth reciprocating motion without reversing the direction of rotation of the drive motor. A rotary ferrofluidic feedthrough (Ferrofluidics Corp., Nashua, NH) couples the gearmotor to the ball reverser, which is housed in the helium gas of the magnetic piston circuit. This eliminates the requirement for reciprocating vacuum seals on the piston drive shaft.

The key components of the 4-15 K magnetic refrigerator are the cylinder assembly and the piston containing the paramagnetic material. The cylinder assembly is made of thin-wall stainless steel and provides the ducts through which the heat exchange fluid flows (Fig. 2). The ducts are made from thin-wall rectangular waveguide to minimize the annular gap between the piston and the magnet. The phenolic piston is machined in three parts -- two thin-wall cups to contain the porous $Gd_3Ga_5O_{12}$ (GGG) matrices and a solid center section to separate the matrices (Fig. 2). Threads were cut into each piece to facilitate both the assembly of the piston and the modifications to the matrices. Each compartment is 33 mm long and 38 mm in diameter and is filled with 160 gm of 1.1 mm diameter GGG spheres for a fill factor of about 60%. Stainless screens are inserted in each end of the compartment to prevent the GGG from migrating out the holes in the piston.

The use of the two matrices doubles the heat removal capacity per cycle of the piston and provides a more continuous transfer of heat to help reduce temperature fluctuations. The 4.2 K cooling power of the magnetic stage operating ideally in a Carnot cycle can be given as

$$\dot{Q}_C = nT_C v \Delta S \eta$$

where n is the number of moles of Gd^{3+} in the matrices, T_C is the refrigeration temperature, ν is the frequency of operation and ΔS is the change in entropy during the isothermal demagnetization, and η is the fraction of Carnot efficiency at which the magnetic refrigeration stage operates. In this design there is 0.948 moles of Gd^{3+}, and if the matrix cycles between 0.5 T and 6.5 T over the temperature span of 4 K and 16 K we can assume ΔS is 0.3R (which takes into account the entropy change of the GGG minus the entropy change of the entrained helium gas), then the refrigeration power at 4.2 K is

$$\dot{Q}_C = 9.9\nu\eta \text{ W}.$$

Some of the factors effecting the efficiency are the thermal heat leaks along the cylinder wall and the drive shaft, the heat capacities of the piston and cylinder, and the heat transfer between the gas and the GGG matrices. These factors ccontributing to the loss of cooling power of the refrigerator will be identified and minimized during refrigerator testing. No attempt will be made to calculate these effects here. To minimize the internal heat load due to the entrained helium, the helium gas pressure will need to be kept below about 0.1 MPa.

Helium gas provides the heat transfer between either matrix and the low-temperature source and the high-temperature sink. When the GGG matrix is positioned adjacent to a gas duct in the cylinder, helium gas is forced through the holes on one end of the matrix compartment, through the porous matrix, and out the set of holes on the other end of the compartment (fig. 3). The ridge in the center prevents gas leakage along the outside of the piston. The indents in the outer surface of the piston allow the gas to flow through the matrices while the displacer is still in motion so that gas flow need not be limited to the time the piston is positioned at the ends of the stroke. The placement of the gas ports in the cylinder and the geometry of the piston eliminate the need for mechanical valves at these low temperatures. During this portion of the cycle the refrigerator operates in an isothermal fashion. As the piston is then moved from one end of the stroke to the other, the outer ridges of the piston act as close tolerance seals to prevent the gas from either circuit from passing along the cylinder wall and thermally short-circuiting the matrices. The low-friction fiberglass-impregnated teflon seals further insure that the gas leakage is minimized. This allows the matrices to magnetize or demagnetize in an adiabatic fashion. Thus the cycle of the piston should approximate the Carnot cycle.

Heat exchangers filled with phosphor-bronze screens are used to transfer heat between the helium gas in the circuits and the heat source or the heat sink. Fluid flow through the gas circuits is produced by separate linear-induction, positive-displacement pumps in both the low- and high-temperature gas circuits. The two gas pumps are driven back and forth in phase relation to the motion of the GGG piston. The pumps easily develop the low pressure head required to overcome the pressure drop through the GGG matrices and the heat exchangers. These pumps have been operated successfully at low temperatures but their long-term performance has not yet been determined.

3. Component Test Results

The use of the Hiperco surrounding the magnet provides a more rapid transition between the high field and low field regions enabling a shortened stroke length for the GGG piston. Figure 4 compares the measured axial magnetic field profile of the solenoid with and without the Hiperco and shows the position of the piston at the end of the stroke. At either end of the stroke, the axial field at the position of the center of the two GGG matrices is 0.5 T and 6.5 T, with a maximum ±7% change in the measured axial field over the length of the GGG matrix in both the high-field and the low-field regions.

The magnetic field pulls both GGG matrices towards the center of the magnet. The magnitude of this attractive force depends on both the magnitude and gradient of the magnetic field which, for cylindrical symmetry, may be approximated by $F_z = m_z\,(\partial Bz/\partial z)$, where F_z, m_z, and B_z are the axial components of the force, the GGG magnetization and the magnetic field, respectively. The use of the Hiperco to shape the 7 T field has generated a magnetic field gradient of 105 T/m which produces a force as high as 1550 N on each of the 160 gm GGG matrices at 4.2 K. This large force dictates the need for careful positioning of the matrices to provide adequate force balancing. From the force equation the first choice made was to position the matrices so as to coincide with

the distance between the maxima in the field gradient. Figure 5 shows the measured force required to move the 4.2 K piston through the magnetic field, with the maximum net force being measured as 630 N. This force could be reduced by decreasing the separation distance between the two matrices. This reduction in force is desirable to reduce the power needed to drive the piston. However the matrices then move through a different portion of the magnetic field profile which will have an unknown effect on the refrigerator perfo.mance. These effects will be examined during testing of the magnetic refrigerator. Additional force compensation, if needed, may be provided by imbedding small slugs of GGG in the center section of the piston so as to be thermally isolated and not a part of the refrigeration process.

4. Conclusion

The high reliability of the individual components should result in a high reliability for the magnetic refrigerator as well. The gearmotor has been overdesigned to handle the anticipated large loads for smooth operation at slow speeds. Operation at these slow speeds will minimize the wear rate on the low-temperature sliding seals. The magnetic refrigerator has been designed to minimize the problems associated with gas contamination. The magnetic refrigerator stage is a closed gas loop system; the gas circuit is sealed after the initial charge of helium gas. The internal gas displacers eliminate the need for an external compressor to provide the gas flow. The external and internal portions of the piston drive train are coupled together with a rotary seal to prevent gas contamination entering the circuit along the drive shaft. The magnetic refrigerator also requires no small orifices as with the Joule-Thomson valve, further minimizing the problems associated with gas contamination. Elimination of the Joule-Thomson circuit can reduce the input power requirements for the compressor by about a third.

The design of the reciprocating magnetic refrigerator to pump heat from 4 K to 15 K has been presented. Initial tests to examine the field shaping ability of the Hiperco and to measure the resulting magnetic forces on the GGG piston have been made in an open-cycle dewar. Further testing to reduce the magnetic force through field shaping will be made in the assembled refrigerator so that the refrigerator performance may be measured as well. The magnetic refrigerator is currently being assembled.

The research described in this paper was performed by the Jet Propulsion Laboratory, California Institute of Technology, under contract with the National Aeronautics and Space Administration.

5. References

[1] Van Geuns, J.R., A study of a new magnetic refrigerating cycle. Philips Res. Rep. Suppl. 6:1 (1966).

[2] Nakagome, H., Tanji, N., Horigami, O., Numazawa, T., Watanabe, Y., and Hashimoto, T., The helium magnetic refrigerator I: Development and experimental results. Advances in Cryogenic Engineering Vol. 29, Plenum Press, New York (1984).

[3] Barclay, J.A., Overton, Jr., W.C., Stewart, W.F. and Steyert, W.A., Magnetic refrigeration for 4-20 K applications'. Technical Report AFWAL-TR-83-3120 (Dec. 1983).

[4] Lacaze, A.F., Claudet, G., Lacaze, A.A., and Seyfert, P., Prospects in Magnetic Refrigeration Proceedings of the ICEC10: Paper A1-2, Helsinki (1984).

[5] Deardorff, D.D. and Johnson, D.L., Magnetic refrigeration development. The Telecommunications and Data Aquisition, Progress Report 42-78, pp 49-58, Jet Propulsion Laboratory, Pasadena, CA (July 84).

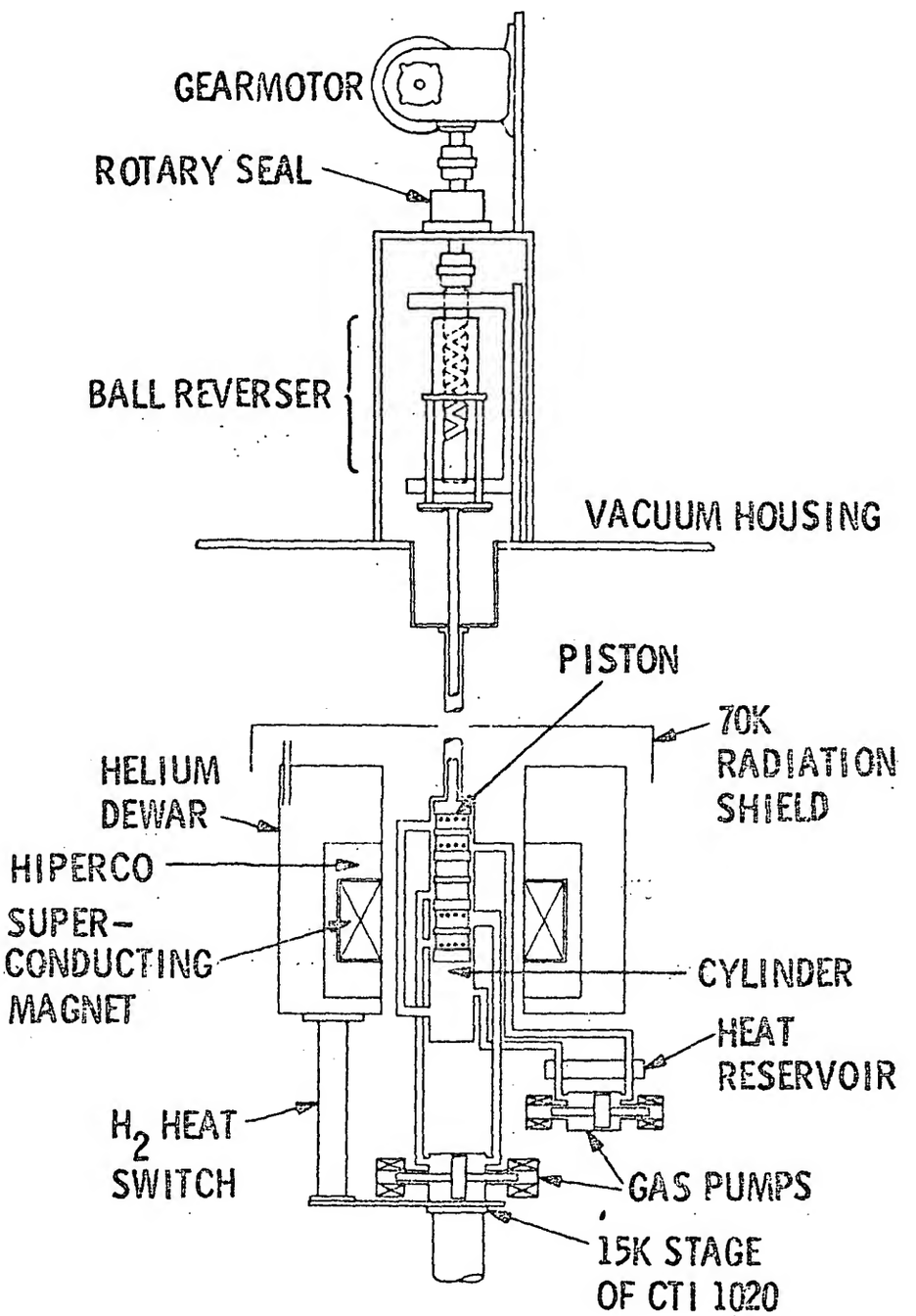

Fig. 1 Schematic of the magnetic refrigerator.

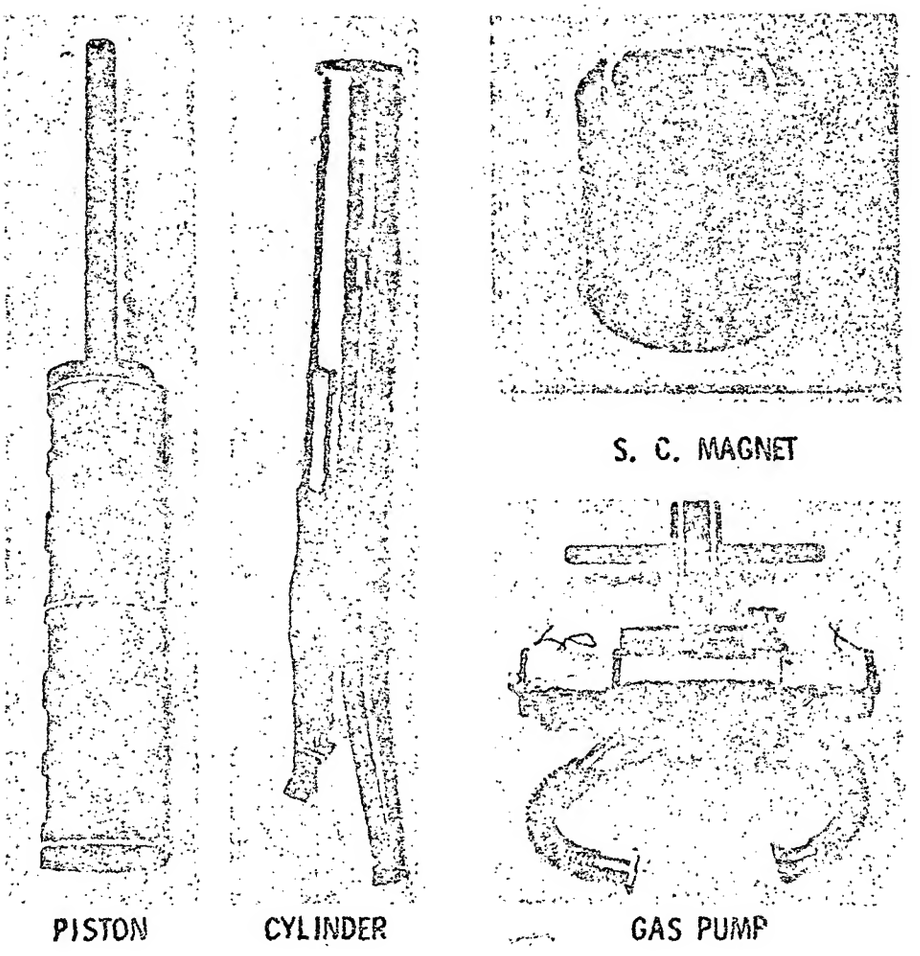

Fig. 2 Magnetic refrigerator components.

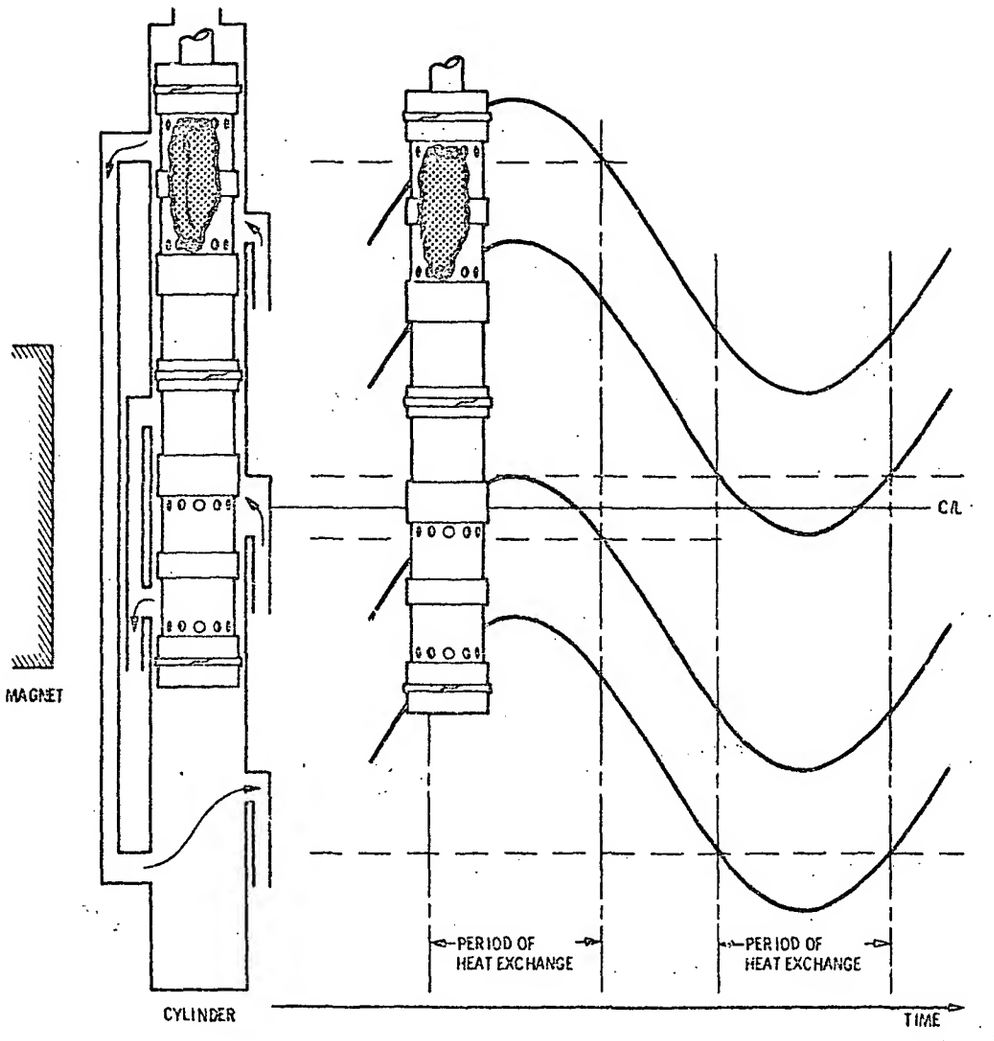

Fig. 3 Schematic showing the time during one cycle of the piston when the indents align with the gas ducts to allow the heat exchange gas to flow through the GGG matrices.

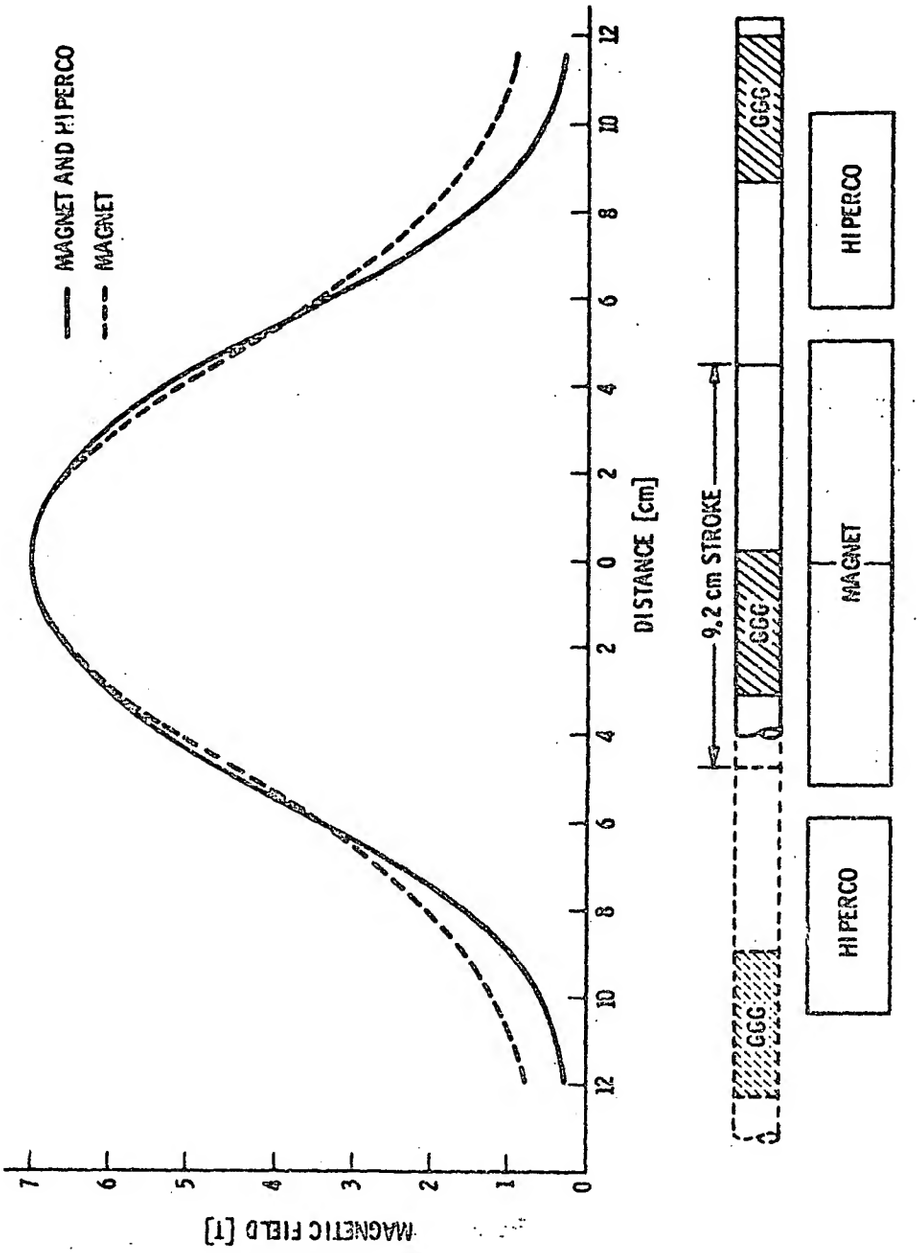

Fig. 4 Comparison of the measured axial magnetic field profiles with and without the Hiperco material. The extreme positions of the piston are shown with respect to the field profiles.

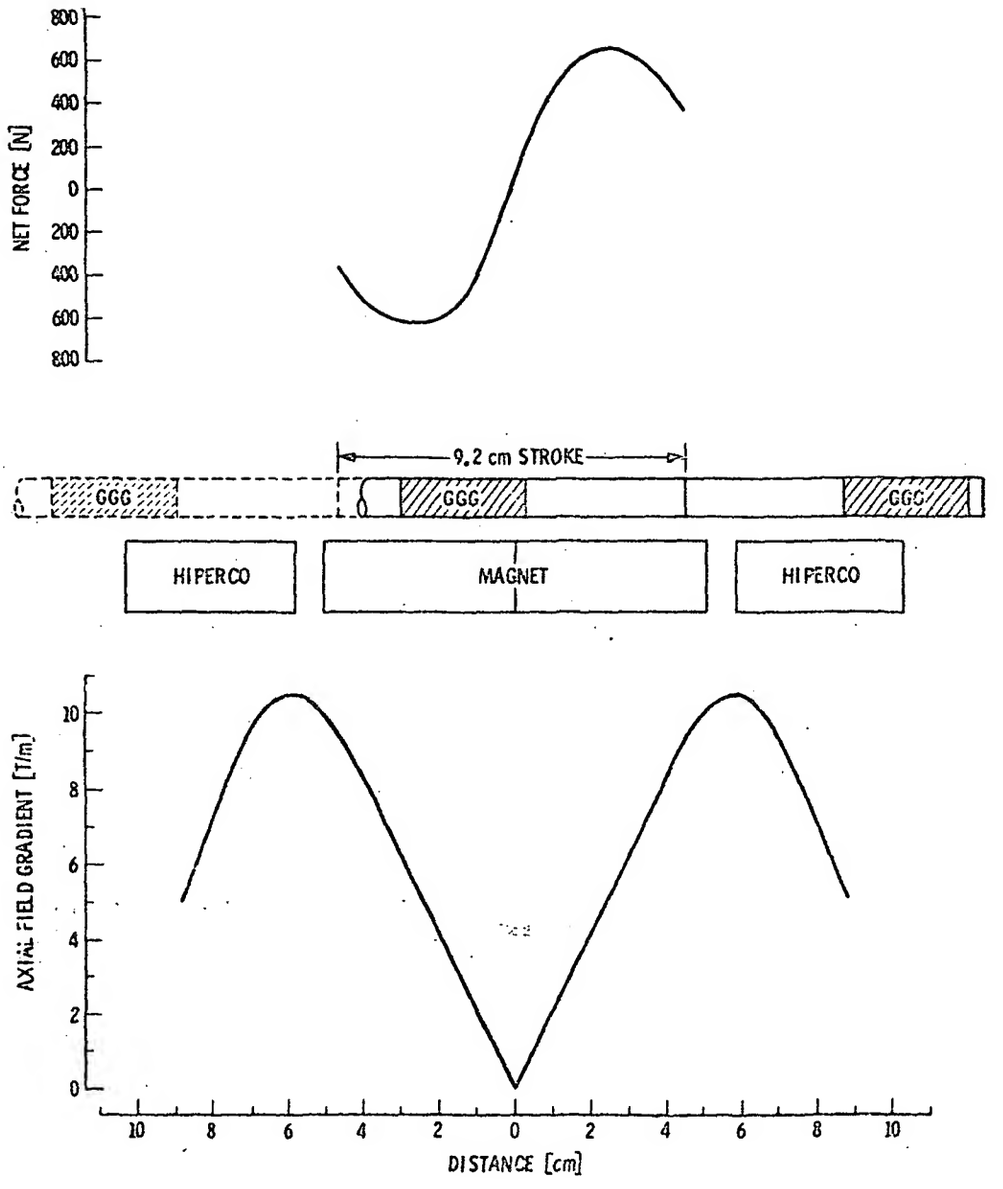

Fig. 5 a) The measured net force required to move the piston through the magnetic field. b) The magnitude of the axial field gradient for the magnet/Hiperco assembly. The extreme positions of the piston are shown with respect to these curves.